A Spatial Processor Model for Object Colour Perception

by G. BUCHSBAUM

Department of Bioengineering, School of Engineering and Applied Science, University of Pennsylvania, Philadelphia, Pennsylvania 19104

ABSTRACT: *A comprehensive mathematical model to account for colour constancy is formulated. Since the visual system is able to measure true object colour in complex scenes under a broad range of spectral compositions, for the illumination; it is assumed that the visual system must implicitly estimate and illuminant. The basic hypothesis is that the estimate of the illuminant is made on the basis of spatial information from the entire visual field. This estimate is then used by the visual system to arrive at an estimate of the (object) reflectance of the various subfields in the complex visual scene. The estimates are made by matching the inputs to the system to linear combinations of fixed bases and standards in the colour space. The model provides a general unified mathematical framework for related psychophysical phenomenology.*

Nomenclature

$L(\lambda)$	illuminant
$R(\lambda)$	reflectance
$\{l_i(\lambda)\}_{i=1}^3$	three dimensional colour space basis that spans $L(\lambda)$ as a linear combination of the basis members
$\{r_i(\lambda)\}_{i=1}^3$	three dimensional colour space basis that spans $R(\lambda)$ as a linear combination of the basis members
$\boldsymbol{\alpha} = (\alpha_1\alpha_2\alpha_3)^T$	vector of coefficients of the linear combination representing the reflectance, $R(\lambda) = \sum_{i=1}^3 \alpha_i r_i(\lambda)$
$\mathbf{v} = (v_1v_2v_3)^T$	vector of coefficients of the linear combination representing the illuminant $L(\lambda) = \sum_{i=1}^3 v_i l_i(\lambda)$
$C_i(\lambda)(i = 1, 2, 3)$	visual system trichromatic colour mechanisms
$\mathbf{y} = (y_1y_2y_3)^T$	vector of trichromatic responses corresponding to a single subfield in the scene $y_i \triangleq \int_{vs} C_i(\lambda)L(\lambda)R(\lambda)\,d\lambda$ (vs = visual spectrum)
$\mathbf{z} = (z_1z_2z_3)^T$	vector of trichromatic responses corresponding to the entire field. $z_i \triangleq \int_{vs} C_i(\lambda)z(\lambda)\cdot\sum_m b_m R_m(\lambda)\,d\lambda$, where b_m is a weighting factor associated with the mth subfield
$\mathbf{h} = (h_1h_2h_3)^T$	internal system standard of field average
κ_{ijk}	$\triangleq \int_{vs} C_i(\lambda)l_j(\lambda)r_k(\lambda)\,d\lambda$
$D(v)$	3×3 matrix, the entries are defined by $d_{ik}(\mathbf{v}) = \sum_{j=1}^3 v_i\kappa_{ijk}$
$Q(h)$	3×3 matrix, the entries are defined by $q_{ij}(\mathbf{h}) = \sum_{k=1}^3 h_k\kappa_{ijk}$
$f_i(\lambda)(i = 1, 2, 3)$	photographing filters defined in the projection experiment
$\boldsymbol{\phi} = (\phi_1\phi_2\phi_3)^T$	$\phi_i \triangleq \int_{vs} f_i(\lambda)L(\lambda)R(\lambda)\,d\lambda$
$p_i(\lambda)(i = 1, 2, 3)$	projection filters defined in the projection experiment

U elementary matrices representing various manipulations of slides in the projection experiment.

The superscript $\hat{}$ on top of a parameter denotes an estimate or internal template parameter of the corresponding actual parameter.

Bold typeface denotes a vector, e.g. **a**; a single vector entry is denoted by its index, e.g. a_i, a_2 etc.

I. Introduction

The large degree of independence of perceived object colour on the illuminating spectrum was already noted by Helmholtz in 1866. He made a clear distinction between surface (object) colour and film colour. The first term refers to colour as a property of a surface and constitutes most of natural colour experience. The latter term corresponds to colour perceived as an expanse of light in a two-dimensional space without objective reference. The term *colour-constancy* is used in this context to define the ability of the visual system to estimate an object colour transmitting an unpredictable spectrum to the eyes. Some of the best known earlier explanations will be mentioned here briefly. However, before going into further details an important comment should be made. The term *constancy* is somewhat misleading. The definition (from Beck (**6**)) is: the approximate constancy of the perceived colour of an object despite changing illumination that alters the intensity and spectral composition of the light stimulating the eye. What this means is that it is not constancy that we are dealing with but rather *inconstancy*. The different accounts, theories, explanations and quantifications are for the changes in perceived hue and other attributes that are caused under different illuminations and context conditions.

Helmholtz (**1**) explained the phenomenon attributing surface colour perception to the presumed ability of the visual system to discount the illuminant. The interpretation of this property in the colour space is that it represents a shift of the achromatic point defined by the average reflectance of the scene. In other words, the scene itself establishes a reference for the visual system. No exact knowledge of the illuminant is needed, the *context* of the scene is important. The problem of how the visual system arrives at object reflectance without prior knowledge of the illuminant is one of the central issues in the various approaches. The implicit estimate of the illuminant on that basis is paramount in the present theory and a very significant issue in the discussion.

One of the outstanding formulations is Helson's (**10**, **11**) adaptation level theory. The major assumption is that colour is detected with respect to a single reference level common to the entire complex field, that is referred to as an *adaptation level*. The adaptation level is the perception that corresponds to an average gray and is a weighted function of the reflectances constituting the complex visual field. The adaptation level is different for different scenes. The very substance of Helson's explanation is stated in the following principle: samples whose reflectances are above the adaptation level increasingly take on the hue of the illuminant; samples below the adaptation level increasingly take on the hue of the complementary afterimage of the illuminant, and samples at

the adaptation level appear achromatic. The basic problem of course is to formulate a systematic algorithm that predicts the adaptation level which incorporates gross spatial context factors of visual field.

Judd (**14**) proposed a quantified version of the adaptation level theory on the basis of Helmholtz's principle of discounting the illuminant and on Helson's principle stated above. The reflectance pattern of the scene provides the information about the illuminant and it is proposed that the average chromaticity of the reflected light is identified with the illumination chromaticity. The average chromaticity is taken to be average (medium) gray. The interpretation is geometric in terms of shifting the reference achromatic locus in a chromaticity diagram. The change in the perceptual attributes corresponds to changes in geometrical distances and orientations. The experimental foundation of the theory consists of hue, saturation and lightness estimation for colour samples under different illumination conditions. The estimation is done by assigning hue, chroma and value according to the Munsell colour scale. For surfaces uniformly illuminated Judd's empirical formulae reach fair levels of accuracy. Additional experiments based on computer generated samples by Pearson *et al.* (**26**) proved successful too. The colour samples in the last experiment comprised only two colour primaries; the importance of this fact will soon become clear to the reader. Additional experiments reported before and after this theory appeared demonstrating additional aspects of the surface colour problem. It was found that the field size relative to the total complex scene is a significant factor. The effect of contrast and field contours on constancy has also been tested. Beck (**6**) presents a comprehensive review of these results. Many of these effects are of a qualitative nature and quantitatively very difficult to measure. In certain cases the scaling is next to impossible, particularly when aspects of cognition were tested.

Land (**16–18**) in a series of projection experiments under special conditions raised again the central issue of the colour processing problem—the strategy and rules applied by the visual system to detect the colour attributes of a reflected spectrum. Using two black and white slides photographed through coloured filters and then projecting these through coloured filters (not necessarily the original photographing filters), Land demonstrated the following basic results:

(a) Almost full colour was recreated projecting with two primaries only (which could not be explained whatsoever by classical colour mixing).

(b) Placing a neutral density filter in front of one projector did not affect much the perceived hue over a broad range of attenuation. (This case is referred to as "projection out of register".)

(c) Projecting through different narrow band filters gave a broad range of perceived colours.

(d) In some defined cases of functional relation between the slides the full "gamut" of hues did not appear, only colours corresponding to simple colour mixture were seen. (These cases are referred to as "achromatic".)

(e) When the records (slides) were interchanged (i.e. the record photographed through the long-wave filter was projected through a short wave filter

and vice versa) a reversal condition appeared. That is, red appeared green, etc., although the reversals were not necessarily the complementary hues.

The results of Land and his associates are mentioned here in detail because they provide an extensive experimental basis for the model we present later. Land found it necessary to introduce a new theory—the Retinex theory of colour vision—to account for his results. The novelty is that the visual system incorporates in addition to the classical filter transformations, a strategy for processing colour. The system incorporates certain normalization and scaling algorithms that allow it to correctly detect hue independently of the transmitted spectrum. The Retinex theory does not require the ability of the visual system to compute the illuminant or make assumptions on its spectral composition. In an additional series of experiments, the Mondrian experiments, Land (**19**) and McCann *et al.* (**22**) clearly demonstrated the constancy of perceived hue under different illuminations giving an account in terms of the Retinex principles. In the Mondrian experiment, a scene composed of different coloured rectangles similar to a Mondrian painting was illuminated by coloured projectors. Technically, it was arranged that, in different presentations, different rectangles having different reflectances will transmit to the eye the same radiance as measured through fixed filters corresponding to the retinal colour mechanisms. The subjects in these demonstrations were able to detect the true colours of the rectangles. An important result is that when the rectangular subfields in question were viewed through a narrow tube isolating them from their context they did not retain their object hues (**19**). Experiments concerning surface brightness constancy and effects of spatial arrangement are reported by Wallach (**29**) and earlier [reviewed in Beck (**6**)] and in recent demonstrations, see Gilchrist (**7, 8**). Land's results raised a fierce debate in scientific literature, see Judd (**15**), Land (**18**), Walls (**30**) and Wheeler (**31**), the basic issue being whether a new theory of colour perception was needed. Jameson and Hurvich (**12**) attribute many of the results to simple effects of colour-contrast. We will not enter into this debate here, but rather leave room for it in the discussion section. However, we should state here that our view is that a large gap in understanding underlies each of the different approaches discussed. A perspective from the systems engineering point of view may clarify the difference between a geometric transformed presentation and an algorithmic processing approach. Models of visual processing that incorporate spatial characteristics of the human visual system and relate visual models to current views on image processing are presented by Hall and Hall (**12**) and Stockham (**27**). The theory we present lacks, as yet, the back-up of appropriate experimental data quantified in terms of its parameters. Therefore, although it presents mathematical derivations and calculations, it is qualitative in nature. But it incorporates and employs principles of communication engineering that allow some generalizations and possible narrowing of the differences and gaps among the views. It demonstrates that under some stated general conditions concerning the scene and the illuminant, colour constancy is achieved. This provides a unified understanding for many results, particularly those of Land, and offers a basis for a comprehensive quantititive theory of object colour.

The basic assumption of the theory presented here is that the central visual processor is recognizer of patterns supplied by the priphery. Given a basis in a three-dimensional colour space and an internal standard field-average, the system arrives at the illuminant spectrum which is subsequently used to compute the reflectance of each subfield in the complex scene. The general idea of pattern and template matching as a basis to account for other colour vision phenomena has been demonstrated earlier [Buchsbaum (**3**), Buchsbaum and Goldstein (**4, 5**)]. The present report is in line with this general approach.

II. Formulation of the Model

A general scheme of the model is presented in Fig. 1. The gross features of the model are the peripheral retinal filters $B(\lambda)$, $G(\lambda)$, and $R(\lambda)$, so assigned according to their wavelength-band response, and two processing phases. The assumption on three retinal colour mechanisms is essentially common to all colour theories and well supported physiologically [Brown and Wald (**2**), Marks *et al.* (**21**)] and psychophysically [e.g. Wald (**28**)]. The approximate position of the filters on the wavelength axis is indicated. Different subfields may stimulate different such colour channels, according to their spatial arrangement, that are, however, of the same wavelength characteristics.

Then, we argue that to get a correct estimate of the object colour properties the system makes an estimate of the illuminant which is assumed to be uniform over the visual field. The illuminant estimate depends on processing of information from the entire field. Then the reflectance of each subfield is computed taking into account the computed illuminant. The assumption of uniformity of the illuminant can be broken down into local uniformity within different areas of the visual field. It is also assumed here that the subfields are as well defined as are the rectangles in Land's Mondrian scenes. In a natural scene the visual system must have its own basis for defining subfields; however, this issue is outside the present scope of this work. The additional fine features and details of the model in Fig. 1 will be discussed throughout this section.

Since the visual system is trichromatic, i.e. has three independent colour mechanisms, and far as it is concerned an arbitrary illuminant or reflectance can be represented with a third order basis set [see e.g. Wyszecki and Stiles (**33**)].

The luminance is represented as

$$L(\lambda) = \sum_{i=1}^{3} v_i l_i(\lambda), \tag{1}$$

and the visual system estimates it as

$$\hat{L}(\lambda) = \sum_{i=1}^{3} \hat{v}_i l_i(\lambda). \tag{2}$$

The reflectance of each subfield is represented as

$$R_m(\lambda) = \sum_{i=1}^{3} \alpha_{im} r_i(\lambda), \tag{3}$$

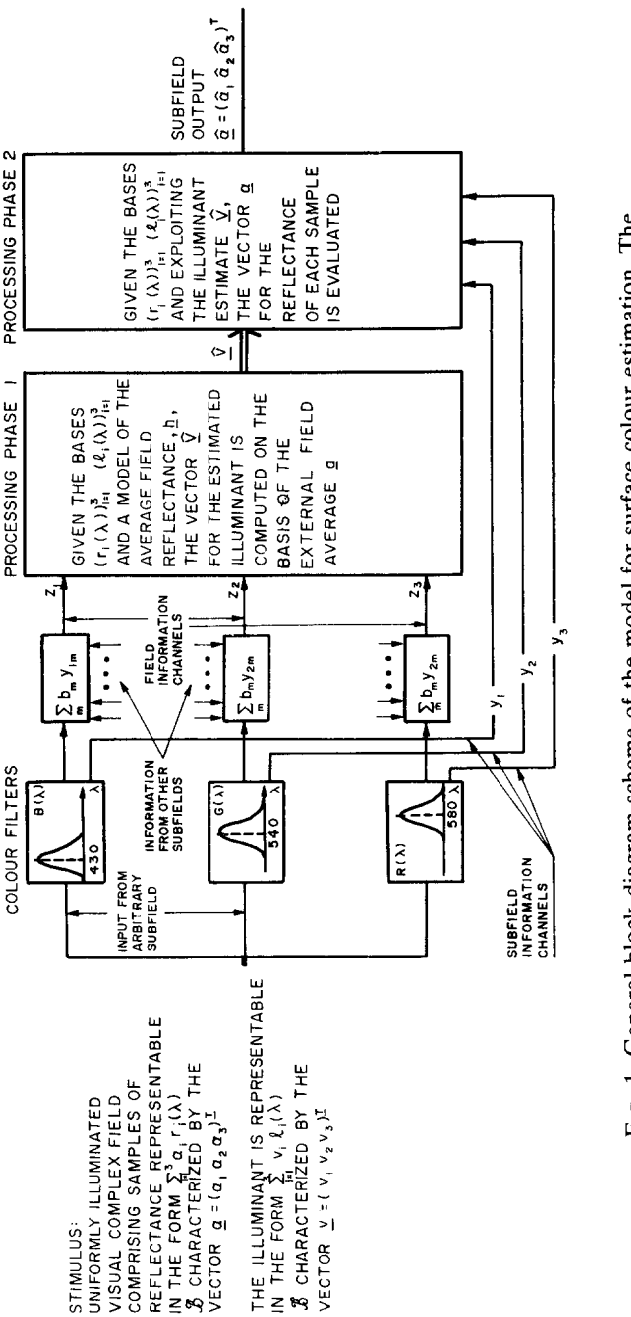

FIG. 1. General block-diagram scheme of the model for surface colour estimation. The stimulus as specified in the text and described at the left side of the figure feeds into three colour filters. These colour filters constitute the basic trichromatic unit channel for the model. Different subfields may stimulate different such colour channels according to their spatial arrangement, that are, however, of the same wavelength characteristics. Phase 1 of the processing exploits a weighted field average of the subfield to arrive at the illuminant estimate $\hat{\mathbf{v}}$. This is done under the assumption that the entire field has a standard average $\mathbf{h}$, that may be different from its true average $\mathbf{a}$. In the second phase of processing, the response of each single subfield together with the estimated illuminant $\hat{\mathbf{v}}$ [are evaluated to get an estimate of the subfield reflectance $\hat{\mathbf{a}}$].

and the visual system estimates it as

$$\hat{R}_m(\lambda) = \sum_{i=1}^{3} \hat{\alpha}_{im} r_i(\lambda). \tag{4}$$

the subscript m corresponds to an arbitrary mth subfield in the scene.

The above notation will accompany this paper throughout. The superscript $\hat{}$ will denote the internally computed parameter by the visual system, of the externally actual corresponding parameter. e.g. $\mathbf{v} = (v_1, v_2, v_3)^T$ represents the real illuminant according to the basis set $\{l_i(\lambda)\}_{i=1}^3$, while $\hat{\mathbf{v}} = (\hat{v}_1, \hat{v}_2, \hat{v}_3)$ is the outcome of phase 1 in the model and is a system parameter. Similarly $\boldsymbol{\alpha} = (\hat{\alpha}_1, \hat{\alpha}_2, \hat{\alpha}_3)$ is a measure of a psychophysical output from phase 2 of the model, while the corresponding vector $\boldsymbol{\alpha} = (\alpha_1, \alpha_2, \alpha_3)$ is a representation of an actual reflectance according to the basis set $\{r_i\}_{i=1}^3$.

The basis functions $l_i(\lambda)$ and $r_i(\lambda)$ $(i = 1, 2, 3)$ are fixed functions and the system's task is to estimate a three-dimensional vector $\hat{\boldsymbol{\alpha}}_m = (\hat{\alpha}_{1m}\hat{\alpha}_{2m}\hat{\alpha}_{3m})^T$ corresponding to the reflectance of the mth subfield in terms of the basis set $\{r_1(\lambda), r_2(\lambda), r_3(\lambda)\}$. That is, for every coloured subfield in the field we get a representation in terms of this basis. (With coloured subfields we include here white, black and all levels of gray, which can also be represented in terms of such a basis.)

Another straightforward constraint is obviously that the set $\{r_i(\lambda)\}_{i=1}^3$ is such that it actually spans the space of coloured visual spectra. This constraint seems trivial and obvious; however, it is important to mention that not every set of three arbitrary spectra can serve as such a basis.

We also require that the visual response to an arbitrary uniform illuminant will be equal to the response to a linear combination of the basis set $\{l_i(\lambda)\}_{i=1}^3$. Thus the subfield's reflectance can be represented by a linear combination of the basis $\{r_i(\lambda)\}_{i=1}^3$. The basis dimension is justified by the trichromatic nature of human colour vision; a higher dimension would give an undetermined set of equations of rank 3. The rank 3 limit applies to cone vision. If rod contribution under special conditions is to be included [McCann (**23**), McCann and Benton (**24**), McKee *et al.* (**25**)] the model dimension would be 4.

The central processor makes a match between the inputs of the colour mechanism and the expected response according to the templates as defined by (2) and (4). For the three independent colour mechanisms, $B(\lambda)$, $G(\lambda)$, $R(\lambda)$ that will be denoted by $C_i(\lambda)$ $(i = 1, 2, 3$, respectively), the trichromatic filter response from each subfield would be (see also Fig. 1).

$$\begin{aligned} y_{im} &= \int C_i(\lambda) L(\lambda) R_m(\lambda)\, d\lambda \\ &= \int C_i(\lambda) \left[\sum_{j=1}^{3} v_j l_j(\lambda)\right] \left[\sum_{k=1}^{3} \alpha_{km} r_k(\lambda)\right] d\lambda \\ &= \sum_{j=1}^{3}\sum_{k=1}^{3} v_j \alpha_{km} \int C_i(\lambda) l_j(\lambda) r_k(\lambda)\, d\lambda \\ &\triangleq \sum_{j=1}^{3}\sum_{k=1}^{3} v_j \alpha_{km} \kappa_{ijk}. \end{aligned} \tag{5a}$$

Note that in the above and all following formulae the integration is over the wavelength visual spectrum. The index m corresponds to a specific mth subfield, the other indices indicate vector elements or basis members.

Also, the integrals of the form $\int C_i(\lambda) lj(\lambda) r_k(\lambda)\, d\lambda \triangleq \kappa_{ijk}$ are fixed system constants and do not depend in the stimulus. The only variable quantities are the illuminant and reflectance vectors $\mathbf{v}$, $\hat{\boldsymbol{\alpha}}_m$ and their corresponding estimates $\hat{\mathbf{v}}$ and $\hat{\alpha}_m$.

Equation (5a) may be put in matrix form

$$\mathbf{y}_m = D(\mathbf{v})\boldsymbol{\alpha}_m \tag{5b}$$

where $d_{ik}(\mathbf{v}) = \sum_{j=1}^{3} v_j \kappa_{ijk}$ are the matrix entries.

The trichromatic responses are internally estimated by an equation of identical form

$$\hat{y}_{im} = \int C_i(\lambda)\hat{L}(\lambda)\hat{R}_m(\lambda)\, d\lambda, \tag{6a}$$

giving a similar matrix equation

$$\hat{\mathbf{y}}_m = D(\hat{\mathbf{v}})\hat{\boldsymbol{\alpha}}_m. \tag{6b}$$

The actual trichromatic response $\mathbf{y}_m$ is equated to the estimate $\hat{\mathbf{y}}_m$

$$D(\hat{\mathbf{v}})\hat{\boldsymbol{\alpha}}_m = \mathbf{y}_m. \tag{7}$$

Equation (7) forms the basic operation of phase 2 (Fig. 1). The known quantity is $\mathbf{y}_m$ and the processor solves the set for $\hat{\boldsymbol{\alpha}}_m$ (in the left wing).

Now we proceed to the key issue of this discussion: how does the system get the estimated illuminant vector $\hat{\mathbf{v}}$, to be used for the solution of (7)? As we can see in all the former discussion, the formulation is symmetric with respect to the illuminant and the reflectance. For every single subfield $L(\lambda)$ and $R_m(\lambda)$ are formally interchangeable.

Here we introduce the basic assumption of this model, which is the following procedure for the estimation of $\mathbf{v}$.

This procedure is similar to the earlier methods used for estimating $\boldsymbol{\alpha}$, but:

(1) The entire visual scene is processed as one unit having a reflectance vector $\mathbf{a}$ that is, a weighted average over the subfield's reflectances.

(2) The system assumes a fixed internal standard reflectance vector, $\mathbf{h}$, for the overall actual field average. The trichromatic response corresponding to the total field would be (see Fig. 1)

$$\int_{vs} C_i(\lambda) L(\lambda) \cdot \sum_m b_m R_m(\lambda)\, d\lambda \triangleq z_i \tag{8a}$$

and by this definition

$$\mathbf{z} = \sum_m b_m \mathbf{y}_m;$$

similarly the field average reflectance vector, $\mathbf{a}$, is

$$\mathbf{a} = \sum_m b_m \alpha_m, \tag{8b}$$

where b_m is a weighting factor assigned to the mth subfield. This weight can be associated with the area of the different subfields, their distance from the centre of the visual field, the shape of the subfields, their orientation and arrangement, etc.

The goal of the system is to estimate the subfield reflectance vector $\hat{\boldsymbol{\alpha}}_m$. Equation (7) cannot be solved for $\hat{\boldsymbol{\alpha}}_m$ without estimated information on the illuminance vector $\hat{\mathbf{v}}$. The basic assumption made, that the system obtains the estimate of the illuminant on the basis of an average taken over the entire field, is now applied. Specifically, it is assumed that the average radiance corresponds to that obtained with the actual illuminance acting on a standard homogeneous field $R_h(\lambda) \triangleq \sum_{k=1}^{3} h_k r_k(\lambda)$. This standard reflectance is assumed by the system to approximate the field average reflectance $\sum_{k=1}^{3} a_k r_k(\lambda)$.

Thus the internal model for estimating the illuminance is

$$\begin{aligned}\hat{z}_i &= \int C_i(\lambda)\hat{L}(\lambda)R_h(\lambda)\,\mathrm{d}\lambda \\ &= \int C_i(\lambda)\Big[\sum_{i=1}^{3} \hat{v}_j l_j(\lambda)\Big]\Big[\sum_{k=1}^{3} h_k r_k(\lambda)\Big]\mathrm{d}\lambda \\ &= \sum_{j=1}^{3}\sum_{k=1}^{3} \hat{v}_j \kappa_{ijk} h_k, \end{aligned} \tag{9a}$$

κ_{ijk} was defined in (5a),

$R_h(\lambda) \triangleq \sum_{k=1}^{3} h_k r_k(\lambda)$ is the system's reflectance standard. Equation (9a) can be put in matrix form

$$\hat{\mathbf{z}} = Q(\mathbf{h})\hat{\mathbf{v}}, \tag{9b}$$

where $q_{ij}(\mathbf{h}) = \sum_{k=1}^{3} \kappa_{ijk} h_k$ are the matrix entries.

The actual trichromatic average response measured by the system is

$$\begin{aligned} z_i &= \sum_m b_m y_{im} = \sum_m b_m \sum_{j=1}^{3}\sum_{k=1}^{3} v_j \alpha_{km} \kappa_{ijk} \\ &= \sum_{j=1}^{3}\sum_{k=1}^{3} v_j \kappa_{ijk} \sum_m b_m \alpha_{km}. \end{aligned} \tag{10a}$$

The above equation can be put in matrix form

$$\mathbf{z} = Q(\mathbf{a})\mathbf{v},$$

where

$$q_{ij}(a) = \sum_{k=1}^{3} \kappa_{ijk} a_k, \tag{10b}$$

and

$$a_k = \sum_m b_m \alpha_{km}.$$

Note that $\mathbf{a}$ is an actual average reflectance vector for the complex field, while $\mathbf{h}$ is an internally assumed standard average.

Equating (9) and (10) gives the equation for estimating the

$$Q(\mathbf{h})\hat{\mathbf{v}} = \mathbf{z}. \tag{11}$$

Equation (11) can be solved for $\mathbf{v}$ which is then substituted into (7) to obtain $\hat{\boldsymbol{\alpha}}_m$ and forms the basic operation for phase 1 (Fig. 1).

What we have here is an adaptation of one procedure (set of equations) to the solution of another procedure. Step 1 is the solution of the set 11. Step 2 is the solution of the set 7, where certain coefficients adjust themselves according to the solution of step 1. It is important to realize that (7) and (11) can be solved to eliminate $\hat{\mathbf{v}}$. The resulting formulation would be a single phase operation that relates the vector $\hat{\boldsymbol{\alpha}}$ to stimulus quantities $\mathbf{v}$ and $\boldsymbol{\alpha}$ only. It could then be seemingly claimed that no estimate of illuminant is made. However, we prefer to give the formulation explicit physical meaning rather than to avoid the critical issue of how the system arrives at the illuminant. (See also the Discussion section.)

Figure 1 summarizes the structure of the model. The stimulus as defined by the model is passed through the filters. The information concerning the entire field (a certain average of the single subfields) is processed to get $\hat{\mathbf{v}}$. This in turn with the information concerning the sole subfields is processed in a second processing phase to get $\hat{\boldsymbol{\alpha}}$ for each subfield. Different subfields are analyzed by similar model units spatially arranged that are not drawn on the figure for reasons of simplification.

III. Primary Results

The two results listed below are theoretically derived; in fact, the model is designed to comply with them analytically: (1) If $\mathbf{h} = \mathbf{a}$, i.e. if the external complex visual field in discussion has a spatial reflectance average that matches the internal standard spatial average, then no matter what the illuminant is, the solution for $\hat{\boldsymbol{\alpha}}_m$ will be equal to $\boldsymbol{\alpha}_m$.

The proof is trivial, in Section II $\mathbf{h} = \mathbf{a} \rightarrow \hat{\mathbf{v}} = \mathbf{v}$ and therefore in $\hat{\boldsymbol{\alpha}}_m = \boldsymbol{\alpha}_m$ irrespective of the illuminant vector $\mathbf{v}$. One has to be careful here to exclude some ill-defined singular special cases, but these do not correspond to any actual practical experiments. The case $\mathbf{h} = \mathbf{a}$ is basic, but most of our discussion and investigation of the model is dedicated to deviations and perturbations from the normal case.

(2) Let us assume a case where two different illuminants, say $\mathbf{v}$ and $\mathbf{v}'$, illuminate the same scene (not simultaneously) or illuminate two different scenes. It may occur then that two different reflectances (each under a different illuminant) will transmit to the eye spectra that will have the same filter outputs (the same vectors $\mathbf{y}$), in terms of the model this means

$$y_{im} = \sum_{j=1}^{3}\sum_{k=1}^{3} v_j \alpha_{km} \kappa_{ijk} = \sum_{j=1}^{3}\sum_{k=1}^{3} v_j \alpha_{kn} \kappa_{ijk} = y_{in}\,, \tag{12a}$$

where the subscripts m, n correspond to the two different subfields. However, under the model solution algorithm with $\mathbf{h} = \mathbf{a}$, the two reflectances will be correctly estimated irrespective of their equal filter output. Conversely, given $\mathbf{v}$,

$\boldsymbol{\alpha}_m$, $\boldsymbol{\alpha}_n$, one can find $\mathbf{v}'$ such that the output of the filters will be equal (for different subfields) but still the estimates $\hat{\boldsymbol{\alpha}}_m$, $\hat{\boldsymbol{\alpha}}_n$ will not be affected, or equivalently perceived hue will not change.

The vectors that correspond to the total field filter response in the two scenes, namely $\mathbf{z}$, $\mathbf{z}'$ are of course not the same as

$$z_i = \sum_m b_m \sum_{j=1}^{3} \sum_{k=1}^{3} v_j \alpha_{km} \kappa_{ijk} \neq \sum_n b_n \sum_{j=1}^{3} \sum_{k=1}^{3} v_j \alpha_{kn} \kappa_{ijk} = z'_i. \tag{12b}$$

Equation (12), however, does not hold if the field consists of only one subfield. This condition can be achieved by viewing the subfield in question through a narrow tube isolating the specific subfield from the context (**19**). Then the two subfields will have the same estimate $\hat{\boldsymbol{\alpha}}$. Furthermore, the estimated reflectance vector, $\hat{\boldsymbol{\alpha}}$, of scenes comprised of one subfield will equal the internal standard $\mathbf{h}$. This follows immediately substituting $\mathbf{a} = \boldsymbol{\alpha}$ (which is the case when a sole subfield constitutes the scene) in (7) and (11).

The experiments implied by these constraints have already been performed. These are the Land "Mondrian" experiments [Land (**18**, **19**) and McCann *et al.* (**21**)] demonstrating hue constancy under different illuminants, with particular subfields having the same integrated absorbed response, **and** the loss of hue when viewing through a narrow tube.

IV. Numerical Analysis and Predictions of the Model

The elements κ_{ijk} correspond to integrals of the bases $\{r_i(\lambda)\}_{i=1}^3$, $\{l_i(\lambda)\}_{i=1}^3$ and the filters $C_i(\lambda)$ $(i = 1, 2, 3)$ over the visual spectrum. Since the outcome of definite integrals of continuous functions is considered there is some freedom in the choice of bases. One possible choice is to take the bases equal to a normalized version of the primaries $C_i(\lambda)$ $(i = 1, 2, 3)$. We have chosen the coefficients κ_{ijk} such that they correspond to some overlap and interaction between the short-$[C_1(\lambda)]$ and middle-$[C_2(\lambda)]$ wavelength spectral bands, considerable overlap and interaction between the middle-$[C_2(\lambda)]$ and long-$[C_3(\lambda)]$ wavelength spectral bands, and no overlap and interaction between the short-$[C_1(\lambda)]$ and long-$[C_3(\lambda)]$ wavelength spectral bands. This is, in fact, the practical case when integrating a set of colour action spectra relative to the form of the κ_{ijk} terms. That is, an idealized set of normalized primaries is taken to be the basis for the space [i.e. $l_i(\lambda) = r_i(\lambda) = C_i(\lambda)$, $i = 1, 2, 3$].
Then:

$$\kappa_{ijk} = \int C_i(\lambda) C_j(\lambda) C_k(\lambda)\, \mathrm{d}\lambda.$$

The actual numerical values used are

$$\kappa_{111} = \kappa_{222} = \kappa_{333} = 1$$
$$\kappa_{112} = \kappa_{121} = \kappa_{211} = 0.1$$
$$\kappa_{221} = \kappa_{212} = \kappa_{122} = 0.1$$
$$\kappa_{223} = \kappa_{232} = \kappa_{322} = 0.33$$
$$\kappa_{332} = \kappa_{323} = \kappa_{233} = 0.33.$$

All other index combinations vanish. The internal standard average **h** is taken as $\mathbf{h} = (50 \quad 50 \quad 50)^T$: that is, the standard average has equal reflectance from the short-wave, middle-wave and long-wave regions respectively. In the following figures, we employ the model using different vectors **v** for the illuminant and different vectors **a** for the true field average. Using different such vectors we could check the outcome substituting an illuminant vector with a dominant or suppressed term corresponding to an actual illuminant with a dominant or suppressed spectral band. In addition, using different vectors **a**, we could investigate the influence of the total field average on the estimation of a single subfield.

We have used values that are quite extreme. Variation between **a** and **h** in some regions goes up to 50% under different vectors **v**. Also, some of the fixed parameters values for each figure are taken from the extremes. However, we

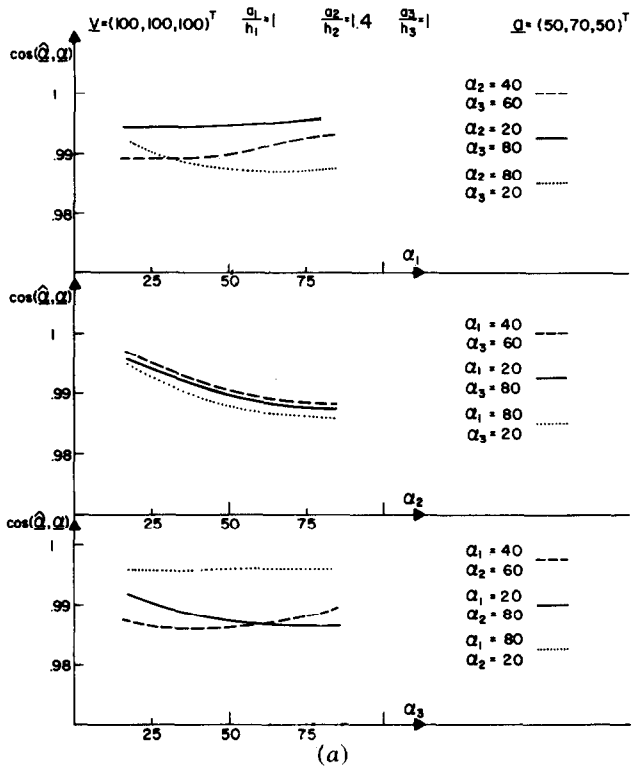

FIG. 2(a)–(c). Model calculation of the cosine of the phase angle between the true reflectance vector $\boldsymbol{\alpha}$ and the estimated vector $\hat{\boldsymbol{\alpha}}$, plotted for different illuminants, $\hat{\mathbf{v}}$, and field averages, **a**. The ordinate indicates the cosine value. The abscissa corresponds to a continuous change of one of the elements of the vector $\boldsymbol{\alpha}$, while the two other entries are fixed parameters. Extreme $\boldsymbol{\alpha}$ values are chosen in some cases to show that in a broad range of conditions the correlation between $\hat{\boldsymbol{\alpha}}$ and $\boldsymbol{\alpha}$ is very high. In this figure and in each of the following, the illuminant vector **v** and field average vector **a** are indicated on the figure. Also are indicated the ratios of the corresponding entries in **a** and **h**. **h** is always taken as $(50 \quad 50 \quad 50)^T$.

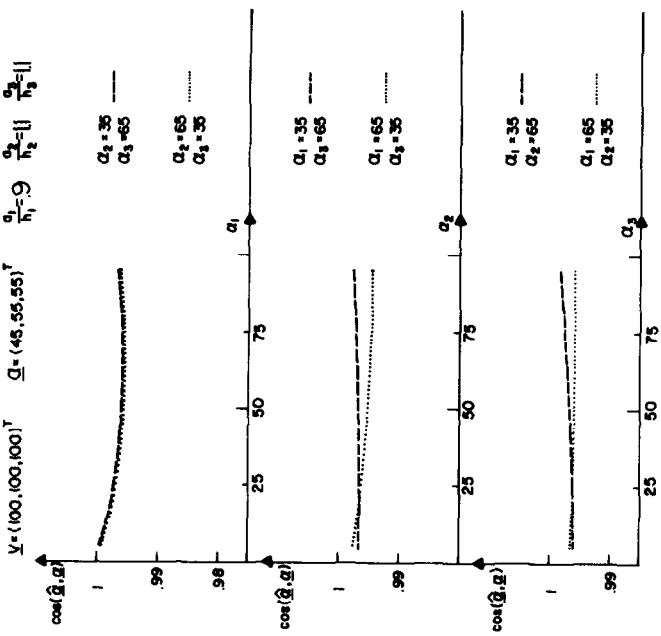

FIG. 2(c)

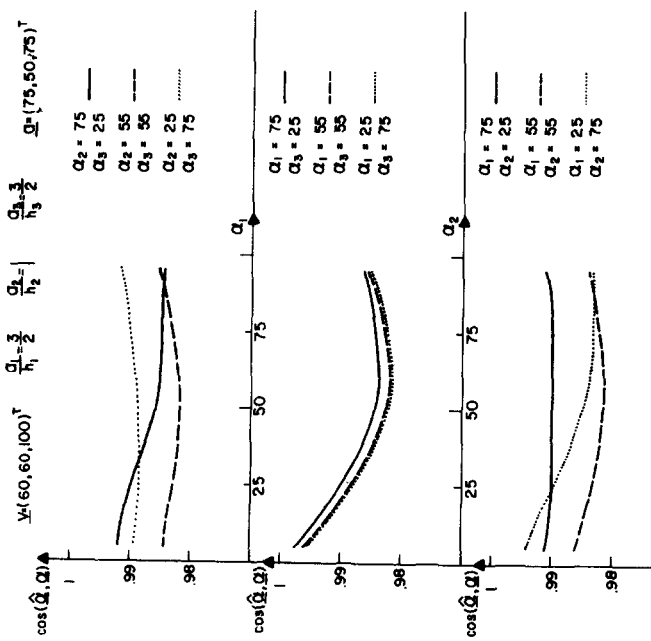

FIG. 2(b)

conclude that no critical distortion in the vector orientation results from these deviations of the true average **a** from the standard average **h** [Buchsbaum (**3**)]. Only a capsule of the numerical calculations is presented in the following figures.

The ordinate on Fig. 2 corresponds to the cosine of the phase angle between $\boldsymbol{\alpha}$ and $\hat{\boldsymbol{\alpha}}$ in different conditions. The abscissa indicates a continuous change in one of the entries of $\boldsymbol{\alpha}$, (there are three figures for each condition) while the other two serve as fixed parameters. In most cases, the two entries that serve as fixed parameters have three different value-pairs so in total each condition has nine curves representing it. On top of each figure are given the vector **a** (true field average vector) which differs from the vector **h** (standard field average vector) which is kept constant, $\mathbf{h} = (50 \quad 50 \quad 50)^T$. Only **a** different from **h** is considered, for otherwise $\boldsymbol{\alpha}$ and $\hat{\boldsymbol{\alpha}}$ would be equal. The relation between **a** and **h** essentially governs the distortion and if these two are reasonably close then the correlation in orientation of $\boldsymbol{\alpha}$ and $\hat{\boldsymbol{\alpha}}$ is very high [Buchsbaum (**3**)].

Figure 3 presents the actual outcome of the model on two-dimensional maps. This is necessary since from the former figures we could learn that the estimated vectors are not too biased in orientation, however, we could not learn in what direction the bias goes. It would be of use to know whether the bias goes in the direction of the field average, **a**, or against it.

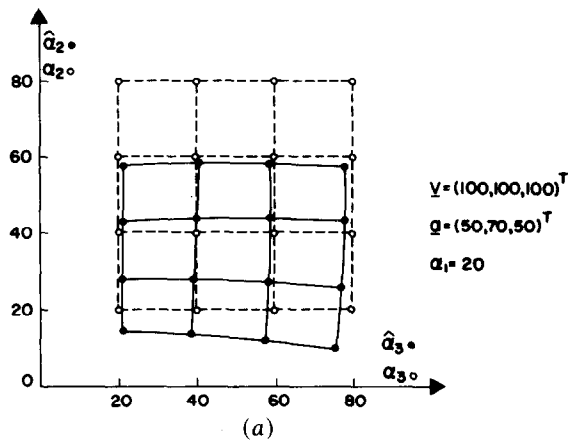

(*a*)

FIG. 3(a)–(c). Model calculations demonstrating the mapping of true reflectances $\boldsymbol{\alpha}$ to their biased estimates $\hat{\boldsymbol{\alpha}}$ resulting from differences between the true and standard average reflectances **a** and **h**. Two of the reflectance vector entries and their corresponding estimates are indicated on the axes, the third entry is a fixed parameter. The open circles indicate points corresponding to $\boldsymbol{\alpha}$, the filled circles indicate points corresponding to $\hat{\boldsymbol{\alpha}}$. The former points are connected by broken lines, the latter set of points by full lines. The figure with the lines connecting the points demonstrates the distortion of the entire structure imposed by the field conditions. In this figure $\mathbf{a} = (50 \quad 70 \quad 50)^T$ has the second term pronounced relative to $h = (50 \quad 50 \quad 50)^T$; the deflection as can be seen on the figure is almost entirely in the direction of supressing the second term of $\hat{\boldsymbol{\alpha}}$. This means that the estimated reflectance $\hat{\boldsymbol{\alpha}}$ is biased in a direction that is opposite to the terms inducing and dominating the true field average. The third entry, which is not plotted, stays almost unchanged.

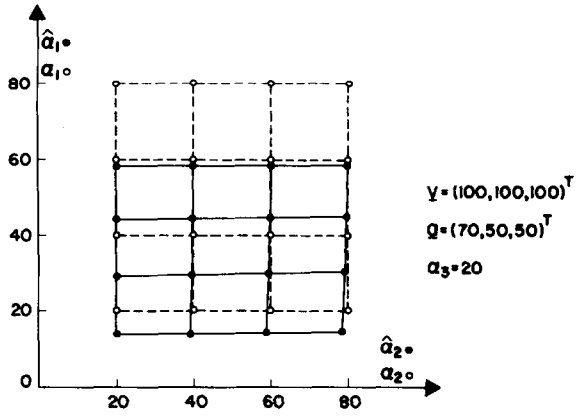

FIG. 3(*b*)

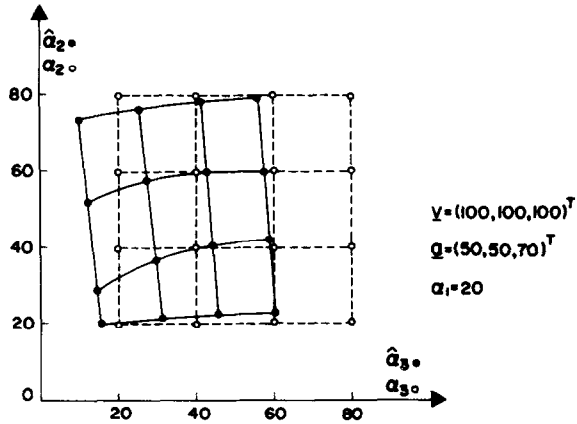

FIG. 3(*c*)

From contrast experiments, see Beck (**6**), it is established that a test-field surrounded by an inducing field has a perceptual impression that tends away from the inducing field. Figures 3(a)–(c) show this effect. In these figures, elements of $\hat{\boldsymbol{\alpha}}$ that correspond to estimated reflectances of different spectral bands are indicated by the filled circles. The open circles correspond to the undistorted true original. Each point represents a possible subfield on a scene with an indicated field average **a**, and illuminated with a certain illuminant represented by **v**. The points constitute two maps and we can see the migration of the different points. The outcome of the model calculation is fully compatible with the experimental observation. In all three illustrations of Fig. 3, the suppressed or deformed band in $\hat{\boldsymbol{\alpha}}$ corresponds to the same band in **a** that is dominant.

V. The Projection Experiment and its Duality with the Reflection Case

In this section, we analyze the performance of the present model in the following reported experimental situation: the scene is photographed through

three coloured filters to generate three black and white slides [Land (**16**, **17**) refers to these slides as records]. The slides are reprojected simultaneously through three coloured filters to reproduce the scene. The photographing and projection filters may (but need not) be the same. A restriction, of course, is that such a set of filters can serve as a basis for the colour space.

Let us denote the photographing filters $f_1(\lambda)$, $f_2(\lambda)$, $f_3(\lambda)$ and the projection filters $p_1(\lambda)$, $p_2(\lambda)$, $p_3(\lambda)$. Each photograph is processed to a black and white slide where each subfield of the scene is transformed to a density of the corresponding subfield on the slide.

This density of the mth subfield on the ith slide has the form

$$\phi_{im} = \int_{vs} L(\lambda) R_m(\lambda) f_i(\lambda)\, d\lambda. \tag{13}$$

Now we can construct the vectors **y** and **z** we defined earlier as the trichromatic responses which serve as the central system inputs,

$$y_{im} = \int_{vs} C_i(\lambda) \left[\sum_{j=1}^{3} \phi_{jm} p_j(\lambda) \right] d\lambda. \tag{14}$$

The vector **z** depends on the average field density of each slide, say $\tilde{\phi}_j$

$$z_i = \int_{vs} C_i(\lambda) \left[\sum_{j=1}^{3} \tilde{\phi}_j p_j(\lambda) \right] d\lambda. \tag{15}$$

With the inputs $\mathbf{y}_m$ and **z** defined, the system equations are formed as in Section II.

If $f_i(\lambda) = p_i(\lambda)$, and the illuminant and reflectances can be represented by the three dimensional bases, then all that is done is a projection (in functional analysis terms) of a vector in a three-dimensional space on a basis in that space and reconstructing it as a linear combination of the same basis. The same set of equations will then solve this case and the normal case discussed earlier. The duality between the two cases can be comceptualized as follows. In the simple reflection case we assumed a common fixed illuminant for the whole scene while the various subfields had different reflectance vectors. In this case the projection spectrum is varied from subfield to subfield according to the density of the slides; however, these projections are reflected from a uniform reflecting screen. Mathematically, the processor solves both cases with the same equations, and so we will find that the projection experiment is most powerful in simulating certain conditions. The projection procedure allows much experimental freedom. The slides can be manipulated in various ways and, in fact, this is the basis for Land's two primary experiments which we reviewed in detail in the introduction section. The manipulation of the slides, or the vector $\boldsymbol{\phi}$, can be represented mathematically by multiplying this vector by elementary matrices. If we denote the elementary matrix as U then the system will solve its equation with the vector $U\tilde{\boldsymbol{\phi}}$ and $U\boldsymbol{\phi}$ controlling its inputs **y** and **z**.

Let us examine a few types of possible matrices U and their implications.

$$\underset{\text{Type 1}}{\begin{bmatrix} a & 0 & 0 \\ 0 & b & 0 \\ 0 & 0 & c \end{bmatrix}} \quad \underset{\text{Type 2}}{\begin{bmatrix} 0 & 1 & 0 \\ 0 & 0 & 1 \\ 1 & 0 & 0 \end{bmatrix}} \quad \underset{\text{Type 3}}{\begin{bmatrix} 0 & 0 & 0 \\ 0 & 1 & 0 \\ 0 & 0 & 1 \end{bmatrix}}$$

$$\underset{\text{Type 4}}{\begin{bmatrix} 0 & 0 & 0 \\ 0 & 0 & 1 \\ 0 & 1 & 0 \end{bmatrix}} \quad \underset{\text{Type 5}}{\begin{bmatrix} 1 & 0 & 0 \\ 0 & 0 & a \\ 0 & 0 & b \end{bmatrix}} \quad \underset{\text{Type 6}}{\begin{bmatrix} 0 & 0 & 0 \\ 0 & 0 & a \\ 0 & 0 & b \end{bmatrix}}, \tag{16}$$

a, b, and c are arbitrary constants.

Type 1 is a multiplication of the entries of $\boldsymbol{\phi}$ by different numbers each. This corresponds experimentally to placing a different neutral density filter in front of each of the projectors.

Type 2 changes the order of the entries of $\boldsymbol{\phi}$. This corresponds to interchanging the slides between the projectors. (With three slides, there are five different such matrices.)

Type 3 zeroes one of the entries of $\boldsymbol{\phi}$. Experimentally it means turning off one projector and using two slides only. This corresponds to Land's two primary experiments.

Type 4 is the same as Type 2, though only the two slides used are interchanged. This corresponds to Land's reversal case.

Type 5 is a case where two of the projectors have the same slide or a multiple of the same slide.

Type 6 is the same as Type 5, but with two slides only; this corresponds to the achromatic case of Land's experiment. Additional combinations that will lead to some new experimental correlates can always be generated.

Figure 4 presents results in a similar format to the earlier cases. The ordinate measures the cosine of the phase angle between $\hat{\boldsymbol{\alpha}}$ and $\boldsymbol{\alpha}$. The abscissa indicates a continuous change of entries of $\boldsymbol{\alpha}$, while the other entries are fixed parameters. In all cases $\mathbf{v} = (100 \quad 100 \quad 100)^T$ and $\mathbf{h} = \mathbf{a} = (50 \quad 50 \quad 50)^T$. The interference matrix U is shown on each figure. In Fig. 6(a) three projections are present though different wedges interfere with them. In major parts of the parameter range the outcome is reasonable compared to cases without interference. In Fig. 6(b) only two slides stay (the second and third entries of $\boldsymbol{\phi}$), those that correspond to the middle and long spectrum bands. We should emphasize that in most cases we present extreme-range fixed parameters values and run the continuous variable over the total range. It is difficult to evaluate exactly what the contribution of every single point is, but over considerable ranges, although distortion will appear, the estimated $\boldsymbol{\alpha}$ will reasonably well, match $\boldsymbol{\alpha}$.

The result is much more striking and evident on Fig. 5 where the complete migration map is presented. Two of the entries of $\hat{\boldsymbol{\alpha}}$ are maintained almost unchanged. The third is always a function of the other two and is not

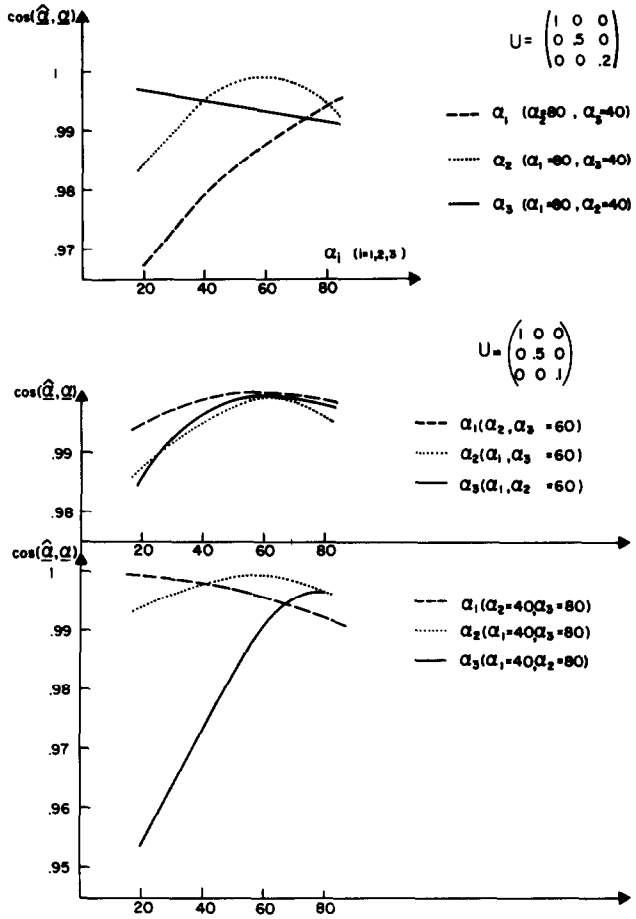

FIG. 4. Cosine of the phase angle between $\hat{\alpha}$ and α is plotted for some conditions of the projection experiment. The ordinate indicates a continuous change in one of the entries of α while the other two stay as fixed parameters. The interference matrix U is indicated together with the rest of the field conditions. Here the interference matrix corresponds to placing neutral density filters in front of two of the projectors. It can be seen that the system does well enough under this distortion and the cosine correlation between $\hat{\alpha}$ and α is still very high.

independent of them (a point soon to be discussed). The open circles correspond to the true α, the filled circles to the entries of $\hat{\alpha}$. This corresponds to the two primary projection experiment (**16**, **17**) and confounds the results.

An interesting map is generated for the reversal experiment. Figure 6 shows that the estimated values (filled circles) form a slightly distorted mirror-image of the original entries (open circles), which describes the outcome of this experiment.

Before we go further, there is an important point to emphasize. The dimension of the estimated vector remains 3 always, but the interference

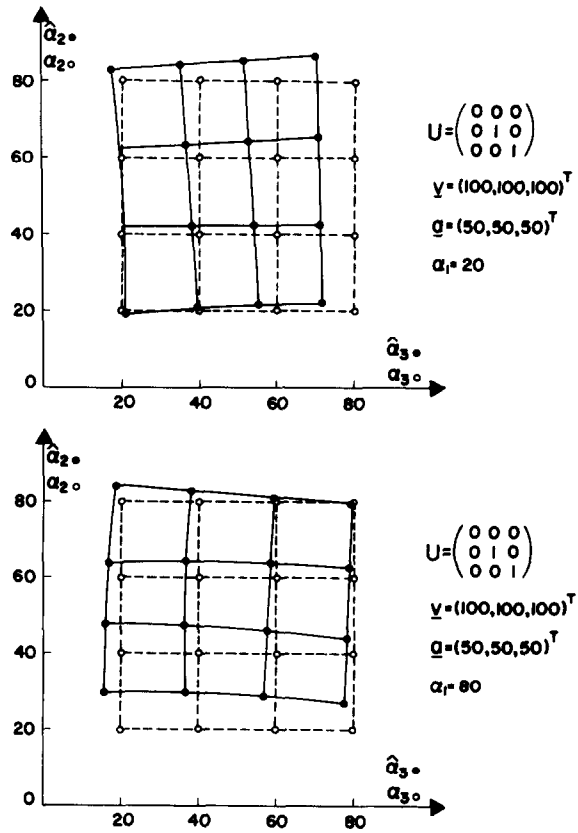

FIG. 5. Bias in estimated reflectance caused by projecting only two records. Two entries α_2 and α_3 are shown on the two dimensional map. The open circles present the true entries and the filled circles the estimated entries. The third entry is a fixed parameter. It seems that with two records only, the system does well; no major deflection is detected. But here one should be careful and bear in mind that the third entry is always dependent on the other two and not independent as earlier.

matrices corresponding to the actual experiment reduce the rank of the equation set into 2. Land (**16**, **17**) reports that it was possible to recreate in the two primary colour experiments almost all of the colours; however, in each case part of the spectrum was missing depending on the projection filters. We conclude from the previous discussion that part of the colour space ought to have been missing because of the reduction of rank. A different part was missing in each case because the projector filters were manipulated. Thus, in a way, this is a kind of simulation of reduced colour vision to a normal trichromat.

The achromatic cases are easy to understand; the set of equations with the interference matrix has rank 1. The solution is of dimension three but all the points lie on a single line in the space. The orientation of the line is determined by the projectors, and only mixtures of the projection spectra will be perceived.

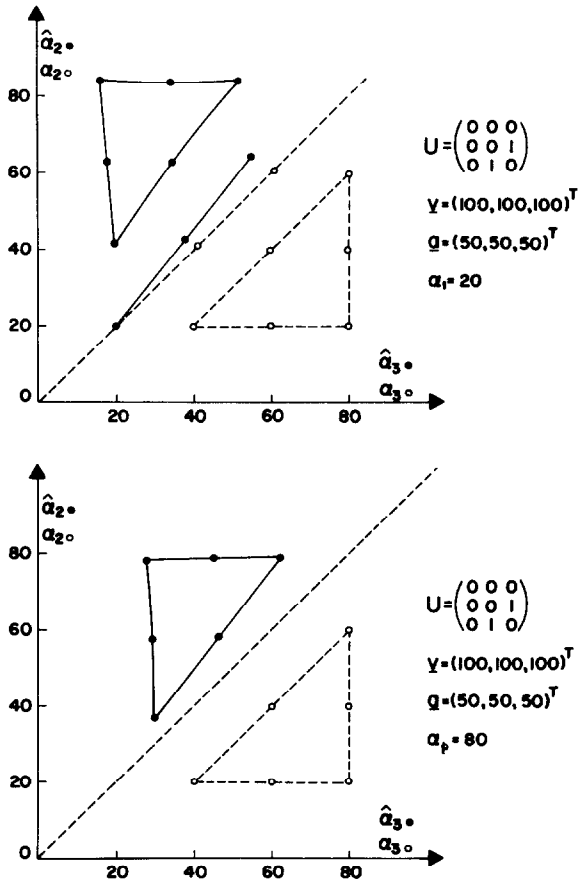

FIG. 6. Migration map of entries of α to entries of $\hat{\alpha}$ when the interference matrix U corresponds to the reversal of two records (the two records are interchanged). The open circles correspond to the true vector entries, the filled circles to the estimated vector entries. The estimated entries constitute a slightly deflected but almost exact mirror image of the true entries relative to an axis that is a 45° straight line through the origin. Some points on this line are also indicated with their image. In numerical terms, this mirroring means that the true entries just interchange their numerical in their image.

VI. Summary and Discussion

This report presents a comprehensive model based on engineering concepts. The model provides a new unified solution for surface colour perception. The model is theoretical but highly correlated and consistent with various experimental results, particularly those of the projection and Mondrian experiments of Land and his Associates [Land (**16**, **17**, **19**), McCann *et al.* (**22**)]. Full compatibility with colour contrast constraints is also demonstrated. A unified understanding is given by the model for the various phenomena and the model is realizable for purposes of critical experimental investigation. Some experi-

mental possibilities are discussed following a brief review of the model principles and results.

The basic assumptions of the theory are:

(a) The visual system implicitly computes the illuminant of the field and the reflectance of each subfield in the scene by matching them to linear combinations of three dimensional bases. The computed (or estimated) values are the scalar coefficients of the linear combination of the basis. The basis members are fixed and the basic constraint imposed on the basis is that it actually spans the colour-space.

(b) The illuminant is assumed common to the entire field. The illuminant estimate is made under the assumption that the visual field in question has a fixed spatial reflectance-average that follows a certain standard, i.e. the system presumes that its standard average reflectance is equal to the actual spatial field average.

(c) A set of linear equations is formed for the illuminant and each subfield; the equations are based on the inputs to the system. These generalized equations [(7) and (11)] are solved for the reflectance vector of each subfield in the various experimental paradigms.

Under these assumptions we have shown using also numerical examples:

1. If the average of the visual field follows the standard, colour constancy is completely maintained. By design of the model, in case of equality between the actual average and the standard, irrespective of the illuminant, the coefficients in the subfield equations adapt themselves such that the solution will be unbiased. All the necessary information on the illuminant exists in the visual field.

2. A bias between the computed reflectance-vectors and the actual reflectances, is introduced in cases of mismatch between the true field average and the standard. However, under a broad range of pertubations from the standard, the bias introduced in the solution is small. Within certain tolerance perceptual constancy will be maintained over a large domain of arbitrary scenes and illuminants. Furthermore, the bias that is introduced when the average and the standard do not match is in the opposite direction of the true field average. This means that an inducing field will cause a perceptual effect on the other subfields away from the inducing field reflectance. This is consistent with colour contrast phenomenology.

3. The model is compatible with observations and findings in the Mondrian experiments by Land (**19**) and McCann *et al.* (**22**). It is shown that two different subfields in the same scene may transmit the same information to the eyes in terms of integrated reflectances (under different illuminations) yet their computed reflectance vector stays unaltered under the overall field processing. The case when a sole subfield is viewed through a narrow tube isolating it from the rest of the context is also consistent and discussed.

4. Under the same set of assumptions, properties of Land's (**16**, **17**) two-primary projection experiment are accounted for. Mathematical duality is proved to exist between the Mondrian experiment and the projection experiment, thus a unified understanding in terms of the same basic engineering

concepts is given to both cases. A convenient representation is given to the various derivatives of the projection experiment, the reversal case, projection out of register, the achromatic cases and combinations of these. Each case is represented by a simple elementary matrix that is introduced in the model equations.

The eariler most outstanding explanations and theories of constancy are those by Helson (**10**, **11**) Judd (**14**) Land (**18, 19**) and McCann *et al.* (**22**). Common to the different approaches is an attempt to account for the perceived colour of a single subfield in terms of the properties of the total complex scene. Helson stated the adaptation principle in which the general idea is that in any arbitrary scene and illuminant, the system adapts and adjusts itself to a certain level. The adaption level corresponds to a stimulus which elicits a perception of medium gray. Sample subfields with reflectances above and below the adaptation level take on the hue of the illuminant or its complementary afterimage respectively. The process we present employs an adaptation idea. For each arbitrary scene and illuminant, the system computes an estimate of the illumination. This is done on the basis of a spatial spectral average of the scene. Once the system gets the illuminant estimate, it readjusts and adapts a set of equations corresponding to the single subfields. Quantitatively, Helson's adaptation level is also determined on the basis of a certain spatial spectral average.

However, in Helson's explanation, the adaptation level, which is an average, partitions the subfields into two groups according to the direction of their hue bias. In the present explanations the field average serves to evaluate the illuminant. Constancy is maintained according to the match or amount of mismatch between the true field average and an image-standard average. The effect of the field average on the perceived hue of single samples is unidirectional—away from the dominating factor in the average—as in simultaneous contrast effects.

Judd (**14**) formulated empirical quantitative rules to evaluate the hue saturation and lightness of surface colour. A geometrical interpretation is given to Helmholtz principle of "discounting the illuminant". This is represented by a shift of the achromatic point on a geometric transformation of the colour space. The formulae are, however, *ad hoc* partitioning of different orientations and distances in that colour space to match the experimental data for hue saturation and lightness. In different experimental conditions, different formulae are used and no systematic quantitative rule is given for these changes of formulae, though each quantification is founded on some empirical findings and the entire theory is phenomenological in nature. The geometrical presentation is an illustration of the meaning of Helmholtz's principle on a transformed colour map. But no further insight on what type of processing is needed to estimate the illuminant and "discount" it, is given beyond the general idea that this is done exploiting clues from the total field average reflectance. The Judd formulae apply only for uniform illuminants. The experimental procedure in Judd's (**14**) report and later in Pearson *et al.*'s report (**25**), that used Judd's formulae, consists of naming hue and scaling of saturation and lightness according to the Munsell system.

The Retinex theory of Land (**18, 19**) and McCann *et al.* (**22**) is inherently different. It is assumed that independent records of the scene are taken through each of the three colour mechanisms. The records are normalized with respect to the brightest spot in each of them. Then the visual system scales each axis of independent triplets computed for each subfield and finally arrives at the reflectances of each subfield. The comparison among the subfields is done by taking the response ratio of adjacent subfields in the short-, middle- and long-waveband records. The scaling of the records in (**22**) involves a transformation of the filters output through a compressive nonlinear psychophysical functions, namely Glasser *et al.*'s (**9**) approximation to Munsel value. The significant advantages of the model are two. The first is theoretical, the Retinex model overcomes the requirement of uniform illuminance. The only additional assumption is that the illuminance is spatially continuous; spatial discontinuities are taken as changes in reflectance. The second advantage is that a systematic realizable algorithm is proposed for the model, that can be implemented choosing an arbitrary sequence of subfields in the scene. However, the scaling algorithm assigns the subfield with maximum lightness in the scene to be white. The existing Retinex examples do not elaborate on cases where this spot varies among the Retinex records or on cases where the maximum lightness spot is not actually white. In the present approach it does not matter whatsoever whether there actually exists a white subfield in the scene or not.

Another account (for some of the phenomena) is given by Woolfson's (**32**) analysis of the two primary projection experiment. His idea is that the system measures the ratio between light reflected from an arbitrary spot in the scene and that reflected from a white spot. This corresponds to measuring the reflectance of an arbitrary spot.

Other approaches that are based on simultaneous contrast effects are also considered (**13**). These are based on the relations among adjacent subfields in a complex scene. Recalling that the Retinex algorithm is a series-product of a sequence of adjacent subfields, it may be debated as to whether the Retinex algorithm is not an implicit generalization of simultaneous contrast effects, and so implicitly bridging the gap between two highly opposing points of view. A possible link between the present approach and the Retinex model can also be found. The set of integrated reflectances [McCann *et al.* (**22**)] used for a quantified calculation of the Retinex examples can be shown to be a linear combination of the reflectance vector $\boldsymbol{\alpha}$ [Buchsbaum (**3**)]. The present model is an idealized processor that can be implemented in various ways. This systems-model does not prefer any one possible algorithm or implementation to another. However, it demonstrates how such an implementation or principle can be unified under a general systems pattern recognizer, constrained by the physical limitations imposed on the visual system.

The issue of estimating the illuminant is very delicate in this context. The computed illuminant is an implicit operation for the visual processor. In fact, the solution for $\hat{\boldsymbol{\alpha}}$ can, in terms of mathematical formality, be made independent of the illuminant extimate; i.e. the estimated reflectance will be a function

of the light reflected from the visual scene (the actual stimulus) and of the processor fixed properties and constant. This is accomplished by substituting (7) and (11) in each other, eliminating $\hat{\mathbf{v}}$. As mentioned earlier, this mathematical maneuver may be the basis for arguing that the visual system does not compute the illuminant. However, we find that an explicit presentation of the operations the external spectrum undergoes is advantageous to conceptually bypassing this intriguing issue. Some theories, particularly the Retinex theory, do not require the system's ability to arrive at the illuminant. We maintain that determining the reflectance of a subfield is essentially the measurement of a transfer function. The reflectance of an object (which determines its colour) is essentially in basic systems engineering terms the transfer function between the illumination as input and the light transmitted to the eyes as output. It is inconceivable that deriving the transfer function on the basis of its output will be independent from any assumption on the input. This means that an algorithm that derives reflectances without explicitly deriving the illuminant nevertheless must have this calculation implicitly built in. Conceptually, we find this in compliance with the old basic principle of Helmholtz, though again it should be emphasized, not its geometrical colour space interpretation. The present model does not "discount" the illuminant but *estimates* it.

The system arrives at the illuminant estimate assuming a certain standard common spatial spectral average for the total field. It seems that arbitrary natural everyday scenes composed of dozens of colour subfields, usually none highly saturated, will have a certain, almost fixed spatial spectral reflectance average. It is reasonable that this average will be some medium gray, which comes back to Helson's principle.

However, we do not rely on the vague hypothesis that this can be done on the basis of reflectance-information from the whole visual field but rather show how this can be done and define a pattern-recognizing technique to do it. The unified explicit mathematical formulation we propose solves the problem in terms of spatial complex field analysis.

Acknowledgment

The author is grateful to Professor J. L. Goldstein of Tel Aviv University for his suggestions and criticism during the course of this work. Extensive use was made of the computer facility of the Biocommunications Laboratory, Tel Aviv University. The author was supported by University scholarships. This paper is based on a thesis submitted in partial fulfilment of the requirements for a Ph.D. degree in the School of Engineering at Tel Aviv University, Tel-Aviv, Israel.

References

(1) H. L. F. von Helmoltz, "Treatise on Physiological Optics", (translated by J. P. C. Southall), Optical Society of America, 1924.

(**2**) P. K. Brown and G. Wald, "Visual pigments in single rods and cones of the human retina", *Science*, Vol. 144, pp. 45–52, 1964.

(**3**) G. Buchsbaum, "Models of Central Signal Processing in Colour Perception", Ph.D. Thesis, Tel-Aviv University, 1978.

(**4**) G. Buchsbaum and J. L. Goldstein, "Optimum probabilistic processing in colour perception, Part I: Colour Discrimination", *Proc. R. Soc.* Vol. B205, pp. 229–248, 1979.

(**5**) G. Buchsbaum and J. L. Goldstein, "Optimum probabilistic processing in colour perception, Part II: Colour vision as template matching", *Proc. R. Soc.* Vol. B205, pp. 249–266, 1979.

(**6**) J. Beck, "Surface Color Perception", Cornell University Press, Ithaca, New York, 1972.

(**7**) A. L. Gilchrist, "Perceived lightness depends on perceived spatial arrangement", *Science*, Vol. 195, pp. 185–187, 1977.

(**8**) A. L. Gilchrist, "The perception of surface blacks and whites", *Scient. Am.*, Vol. 240, pp. 112–125, 1979.

(**9**) L. G. Glasser, A. H. McKinney, C. D. Reilly and P. D. Schnelle, "Cube-root color coordinate system", *J. opt. Soc. Am.*, Vol. 48, pp. 736–740, 1958.

(**10**) H. Helson, "Fundamental problems in colour vision", Parts I and II, *J. exp. Psychol.*, Vol. 23, pp. 439–476 and Vol. 26, pp. 1–29, 1938; 1940.

(**11**) H. Helson, "Some factors and implications of color constancy", *J. opt. Soc. Am.*, Vol. 33, pp. 555–567, 1934.

(**12**) C. F. Hall and E. L. Hall, "A nonlinear model for the spatial characteristics of the human visual systems", *IEEE Trans.* Sys. Man. Cyber., Vol. SMC-7, pp. 161–170, 1977.

(**13**) D. Jameson and L. M. Hurvich, "Theory of brightness and color contrast in human vision", *Vision Res.*, Vol. 4, pp. 135–154, 1964.

(**14**) D. B. Judd, "Hue, saturation and lightness of surface colors with chromatic illumination", *J. opt. Soc. Am.*, Vol. 30, pp. 2–32, 1940.

(**15**) D. B. Judd, Appraisal of Land's work on two primary color projections", *J. opt. Soc. Am.*, Vol. 50, pp. 254–267, 1960.

(**16**) E. H. Land, "Color vision in the natural image. Part I", *Proc. Natn. Acad. Sci., U.S.A.*, Vol. 45, pp. 116–129, 1959.

(**17**) E. H. Land, "Color vision in the natural image. Part II", *Proc. Natn. Acad. Sci. U.S.A.*, Vol. 45, pp. 636–644, 1959.

(**18**) E. H. Land, "The retinex", *Am. Scient.*, Vol. 52, pp. 247–264, 1964.

(**19**) E. H. Land, "The retinex theory of colour vision", *Proc. R. Instn. Gr. Br.*, Vol. 47, pp. 23–58, 1974.

(**20**) E. H. Land, "The retinex theory of color vision", *Scient. Am.* Vol. 237, pp. 108–128, 1977.

(**21**) W. B. Marks, W. H. Dobelle and E. F. MacNichol, "Visual pigment of single primate cones", *Science*, Vol. 143, pp. 1181–1183, 1964.

(**22**) J. J. McCann, S. McKee and T. H. Taylor, "Quantitative studies in retinex theory—a comparsion between theoretical predictions and observer responses to the color Mondrian experiments", *Vision Res.*, Vol. 16, pp. 445–458, 1976.

(**23**) J. J. McCann, "Rod-cone interactions: Different color sensations from identical stimuli", *Science*, Vol. 176, pp. 1255–1257, 1972.

(**24**) J. J. McCann and J. L. Benton, "Interactions of long wave cones and rods produce color sensations", *J. opt. Soc. Am.*, Vol. 59, pp. 103–107, 1969.

(25) S. P. McKee, J. J. McCann, and J. L. Benton, "Color vision from rod and long-wave cone interactions: Conditions in which rods contribute to multicolored images", *Vision Res.*, Vol. 17, pp. 175–185, 1977.
(26) D. E. Pearson, D. B. Rubenstein and G. J. Spivack, "Comparison of perceived color in two primary computer generated artificial images with predictions based on the Helson–Judd formulation", *J. opt. Soc. Am.*, Vol. 59, pp. 644–658, 1969.
(27) T. G. Stockman "Image processing in the context of a visual model", *Proc. IEEE*, Vol. 60, pp. 828–842, 1972.
(28) G. Wald, "The receptors of human color vision", *Science*, Vol. 145, pp. 1007–1017, 1964.
(29) H. Wallach, "Brightness constancy and the nature of achromatic colors", *J. exp. Psychol.*, Vol. 38, pp. 310–324, 1948.
(30) G. L. Walls, "Land! Land!", *Psychol. Bull.*, Vol. 57, pp. 29–48, 1960.
(31) L. Wheeler, "Color matching responses to red light of varying luminance and purity in complex and simple images", *J. opt. Soc. Am.*, Vol. 53, pp. 978–993, 1963.
(32) M. M. Woolfson, "Some new aspects of color perception", *IBM Jl Res. Dev.* Vol. 3, pp. 312–325, 1959.
(33) G. Wyszecki and W. S. Stiles, "Color Science", John Wiley, New York, 1968.